

3D Visualization of Cardiac Anatomical MRI Data with Para-Cellular Resolution

Christopher E Goodyer, Vicente Grau, Tahir Mansoori, J rgen E Schneider,
Ken W Brodlie and Peter Kohl

Abstract—Advances in research and clinical techniques are providing increasing quantities of data at improved spatio-temporal resolution. It is therefore imperative to develop matching approaches for efficient analysis and intuitive presentation of this data. Using the example of advanced magnetic resonance imaging, this article will illustrate the challenges involved in computational reconstruction and interactive visualization of the three-dimensional cardiac anatomy, based on magnetic resonance imaging data with para-cellular resolution.

I. INTRODUCTION

HOMOGENEOUS cardiac performance arises from well-coordinated electro-mechanical activity in a structurally and functionally highly heterogeneous substrate [1]. Detailed insight into the micro-anatomical make-up of the heart would be of great importance for the investigation of cardiac function in norm and disease [2]. Ideally this should be obtained using non-invasive procedures.

Among the non-invasive techniques, magnetic resonance imaging (MRI) holds particular promise to provide data on anatomical features, fibre orientation, movement, and even patho-physiological tissue remodelling. Using state-of-the-art image analysis tools, it is becoming increasingly possible to process MRI data within clinically relevant time-frames, to make predictions relevant for the assessment of cardiac anatomy and function [3]. Under experimental conditions, using high field strength MRI equipment and isolated cardiac tissue, data resolution can be boosted to reach para-cellular voxel dimensions, which opens up new prospects for the discrimination of fine structural detail, relevant for the quantitative description of tissue architecture.

To turn the vast volume of MRI-generated data into user-accessible information, new input-output options need to be considered. This would ideally allow non-technical experts to explore the data-space in real time, and in an intuitively

obvious manner. Here, we illustrate how advanced visual display technologies allow one to manipulate high-resolution MRI data, surface-rendered using an approach based on the freely available Visualization Toolkit (VTK; <http://www.vtk.org/>), and displayed using standard OpenGL (<http://www.opengl.org/>) features.

II. DATA ACQUISITION

Methodological details were described previously [2]. In brief, high-resolution MRI experiments were carried out on an 11.7 T (500 MHz) MR system, comprising a vertical magnet (bore size 123 mm; Magnex Scientific, Oxon, UK), a Bruker Avance console (Bruker Medical, Ettlingen, Germany), and a shielded gradient system (548 mT/m, rise time 160 μ s; Magnex Scientific, Oxon, UK). Dedicated quadrature driven birdcage RF-coils were used to transmit/receive the MR signals. Using a fast gradient echo technique for high-resolution gap-free three-dimensional (3D) MRI, a coronary perfusion-fixed rabbit heart, embedded in agarose, was scanned with an in-plane resolution of 26.4 μ m \times 26.4 μ m, and an out-of-plane resolution of 24.4 μ m. Reconstruction of the MRI data was performed off-line, using purpose written C-software, generating a stack of 2D TIFF-images. In total, 1440 16-bit TIFF images with a resolution of 1024x1024 pixels were used for post-processing (for details see [2]), resulting in approximately 1.5 GB of total data.

III. DATA PROCESSING

Anatomical MRI sections were segmented to accurately discriminate between cardiac structures. For segmentation, plain thresholding of the original datasets is not sufficient, due to intensity variations within and between images. The MRI stack was initially segmented using a combination of level sets and connected thresholding (Fig. 1). Then, mathematical morphology operations were used to fill small holes in the tissue and to eliminate isolated points in the background. A block-wise approach, in which the volume is divided into subvolumes on which the algorithm is applied, was implemented to deal with the huge image sizes. Examples of the segmented slices are shown in Figure 2. Given the limited intensity differences, only tissue and non-tissue (including cavities, vessels and interstitial clefts) classes are currently extracted.

Manuscript received May 25, 2007. Funding for this work was provided by the UK Biotechnology and Biological Sciences Research Council, the Engineering and Physical Sciences Research Council, and the British Heart Foundation.

C. E. Goodyer (e-mail: ceg@comp.leeds.ac.uk) and K. W. Brodlie (e-mail: kwb@comp.leeds.ac.uk) are with the School of Computing, University of Leeds, Leeds, UK.

P. Kohl (phone: [+44] 01865 272114; fax: [+44] 01865 272554; e-mail: peter.kohl@dpag.ox.ac.uk), V. Grau (e-mail: vicente@robots.ox.ac.uk), T. Mansoori (e-mail: tahir.mansoori@comlab.ox.ac.uk), and J. E. Schneider (e-mail: juergen.schneider@dpag.ox.ac.uk) are with the University of Oxford, Oxford, UK.

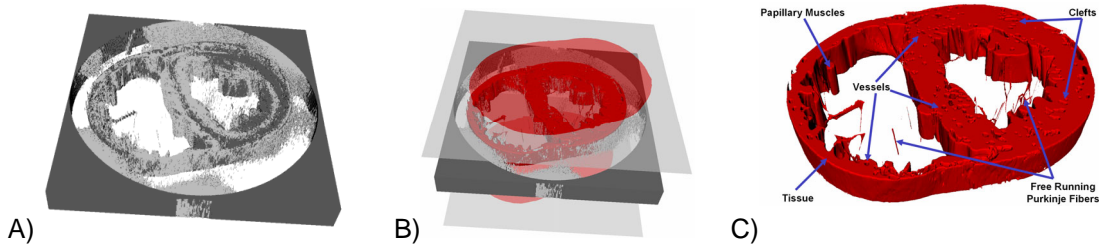


Fig. 1 Segmentation of MRI slices of rabbit heart. A: MRI sub-volume image stack with noise, B: Level set bounding surfaces used to perform threshold connected segmentation, C: Segmented MRI sub-volume stack.

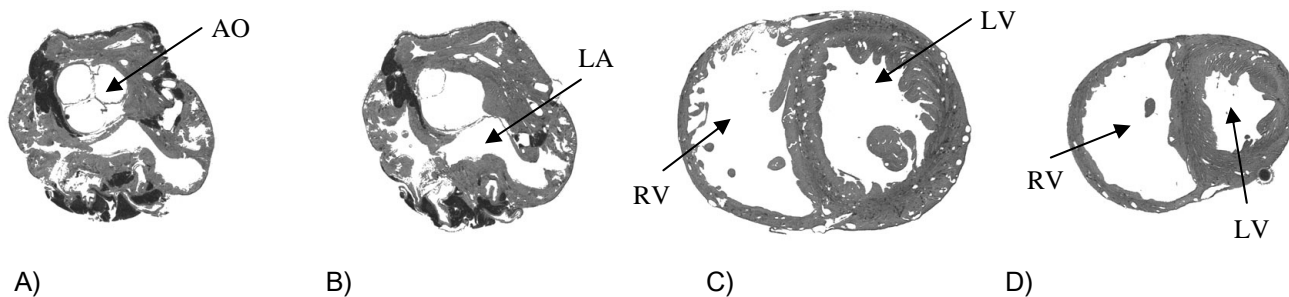


Fig. 2 Examples of segmented MRI slices: individual slices arranged from base towards apex from A to D. AO – aortic valve, LA – left atrium, LV – left ventricle, RA – right atrium, RV – right ventricle.

Using this segmentation process, each voxel is assigned a label, identifying it as either ‘tissue’ or ‘non-tissue’. 3D surfaces that separate the two classes are then built, using isosurfacing, which is the extension of contour mapping into three dimensions. The isosurfacing was performed using the *ContourFilter* routine in VTK. This enables a volume of slices with known physical separation to be mapped.

Surfaces produced by the above procedure tend to be noticeably jagged. This is because the rectangular acquisition grid will tend to generate sharp joints at ‘corners’. This is shown in Figure 3, where a simple set of two-dimensional pixels is shown at the intersection of grid lines. The grey circles show original data that is being interpreted as ‘tissue’, while the white ones are taken to be ‘cavity’ (Fig. 3A). In Figure 3B, an isosurface has been added midway between adjacent pixels of different class, to indicate the boundary. Intuitively this makes sense, as at some point between the two discrete pixels, there must be a transition from tissue to non-tissue.

We also know a-priori that such boundaries are not

normally sharp in biological samples. Thus, by applying a smoothing algorithm (Fig. 3C), we can generate surfaces which follow the overall shape of the data without being constrained by the ‘false precision’ of the boundaries. This smoothing operation is not only important in terms of providing visual realism, but also for subsequent use of data in simulations of cardiac behaviour or external interventions such as defibrillation (which would cause spurious current peaks at sharp changes in surface geometry). It is, however, imperative not to smooth too much, as real features in the data could be lost. This is illustrated in Figures 3D. The effect of smoothing cardiac MRI data on visual presentation is illustrated in Figure 4, where the raw isosurface (Fig. 4A) is compared to the same surface area after 10 iterations of VTK’s *vtkWindowedSincPolyDataFilter* smoother (Fig. 4B).

The final step of data pre-processing is a reduction in the number of triangles used. In smooth sections of geometry it is possible to employ significantly fewer points to map a surface than originally generated. Again, we used VTK for this operation, namely the *DecimatePro* routine, which

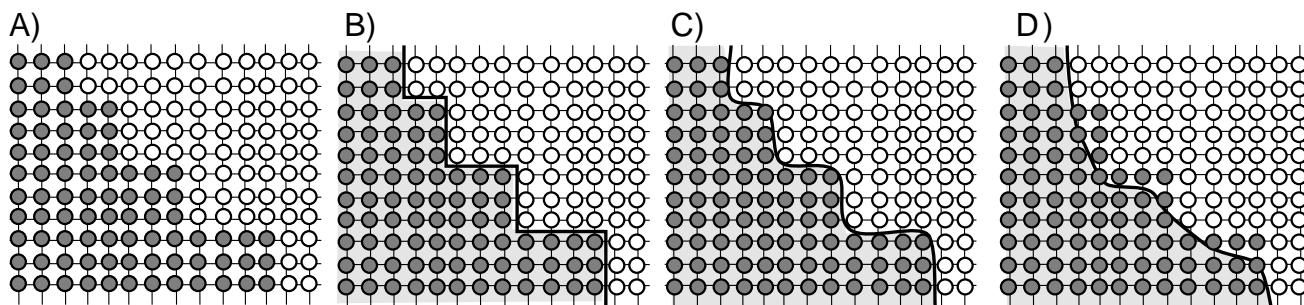


Fig. 3. Schematic illustration of the isosurfacing approach. A: original 2D data points include two classes: tissue (filled circles) and non-tissue (open circles); B: isosurface contour, marking the boundary between different data classes; C: adjusted boundary after careful smoothing; D: boundary after excessive smoothing.

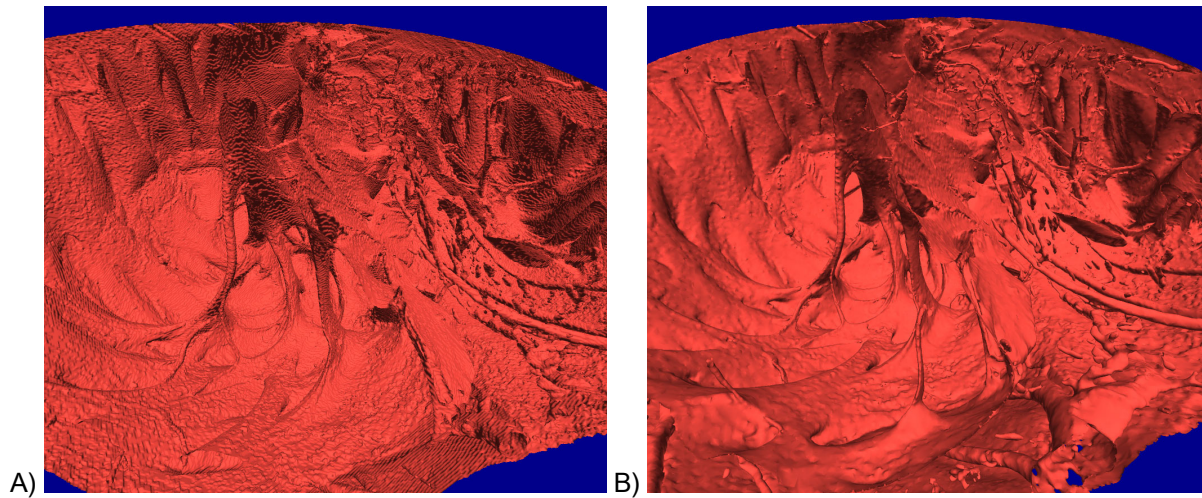


Fig. 4. Effect of smoothing on cardiac MRI data visualization. A: Original isosurface; B: Isosurface appearance after 10 iterations of VTK's *vtkWindowedSincPolyDataFilter*.

(combined with the smoothing) produces good quality surface reconstructions with a reduced number of triangles. For example: Figure 4A shows the original isosurface which contains 6.9 million triangles, whereas in 4B with smoothing and decimation to 80% of the originally generated number of triangles, reduces their overall number to 2.6 million. For the whole heart, this means that a high resolution geometry can be based on 45 million triangles (in this example).

In order to speed-up the rendering routines, we have further post-processed the output files generated by VTK. By reordering the triangle strips into smaller sub-volumes within the entire set, it is possible to write the visualization application in such a way that any section that is not visible in the viewing window will not be processed.

IV. VISUALIZATION

The software package that we have developed loads previously defined surfaces, generated as described above. The advantage of isosurfacing and smoothing during the pre-processing stages is that computationally expensive operations on large datasets will be performed only once, and then loaded as many times as needed for different visualization purposes. This reduces processing times, as loading takes a few seconds, compared to isosurfacing and smoothing which take from minutes to about one hour.

The visualization program employs standard OpenGL features to apply realistic lighting effects for enhanced realism (e.g. Fig. 4B).

Important features implemented for navigation of the datasets include *translocation* along any path in the 3D coordinate system, *rotation*, and *zooming*. Another important navigation technique is the use of an *additional cutting plane*. As opposed to zooming, where the magnification (and hence projection of the data onto the display) changes, a cutting plane allows one to maintain a steady projection area on the screen, whilst revealing successive sections that would otherwise be hidden from view.

The isosurfaces generated correspond to the sum of all interior and exterior surfaces of the heart. These include, on the one hand, small voids within the myocardium (such as interstitial clefts and vessel lumens), and on the other hand, fine structures within the cavities (such as free-running Purkinje fibres and chordae tendinae). In these areas, visual distinction between internal and external volumes can be difficult. To aid intuitive identification of 'in' and 'out', it is helpful to re-apply original MRI images back onto the surface-rendered sections. Even if only one in every hundred slices is projected, this provides good visual cues for tissue identification (compare Figures 5A and B).

Usability of visualizations can be greatly improved by the inclusion of extra data modalities, such as labels and reference points. Labels are an important guide to help users in recognizing structures and locations. Key features are initially identified manually, assigned to a coordinate, and then displayed on screen whenever the relevant coordinate is in the field of view. Reference points are stored as 'way-points', containing viewing position, angle and magnification, to allow one to re-trace a trajectory, or to map out features of interest. Automated transition between these positions allows one to create a continuous 'movie' (a demo is available for download at http://mef.physiol.ox.ac.uk/MRI/3D_Demo.swf).

V. HIGH RESOLUTION DISPLAY WALLS

In order to visually explore large datasets, it is sensible to use the highest resolution for data display possible. We use a system that employs 28 high resolution 20 inch LCD displays, tiled together to form a large (3 m x 1.3 m) drawing surface, also called a 'powerwall'. The displays are arranged in four rows of seven screens, each with a resolution of 1600x1200 pixels, providing a total of about 53 megapixels.

The advantages over a projected display (which could cover a similar physical space) is that LCD displays provide

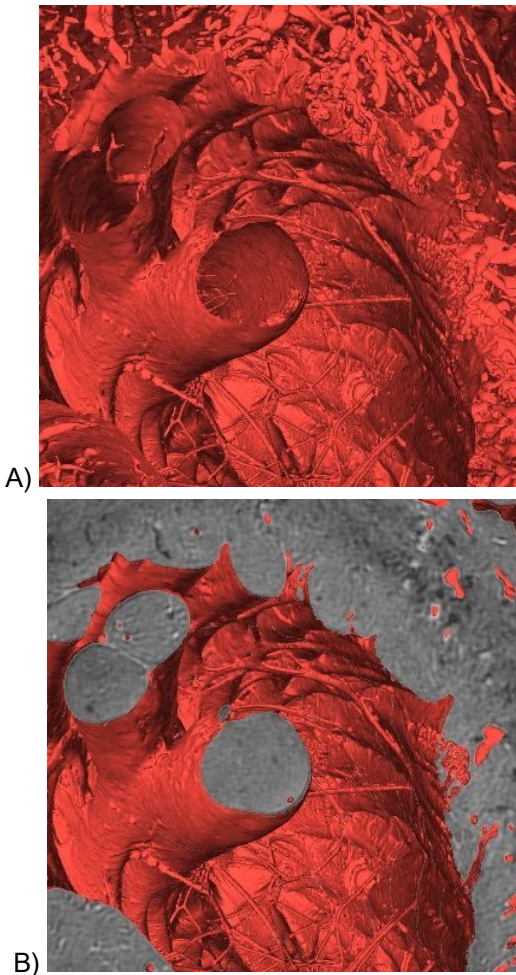


Fig. 5. Left ventricular wall and papillary muscle rendering, viewed from the atrio-ventricular border. A: view of surface rendering only; B: surface rendering (as in A), combined with projection MRI slices that would be in the field of view, to aid distinguishing between tissue and cavity volumes.

a significantly higher resolution of the drawing surface. In addition, unless back-projection was used (which tends to suffer either from reduced image intensity or high cost), the data would be partially obscured during user interaction with the display. In contrast, with the LCD method, the user is encouraged to be relatively close to the wall, since the pixel resolution would be lost to the human eye at larger distances. At the same time, due to the size of the display area, spatial context information is available at all times.

The 28 displays are connected to seven computers, each with two dual-output graphics cards. In order to keep control over costs, standard equipment was used wherever possible. Thus, graphics cards are standard gaming kit (nVidia 7800 GTX), and the screens are regular Dell desktop editions (with the plastic casing removed). The single most expensive item was the custom-made stand that holds the screens in position. The total cost of the system was less than £30,000 (Euro 50,000), which compares favourably with multi-projector solutions [4].

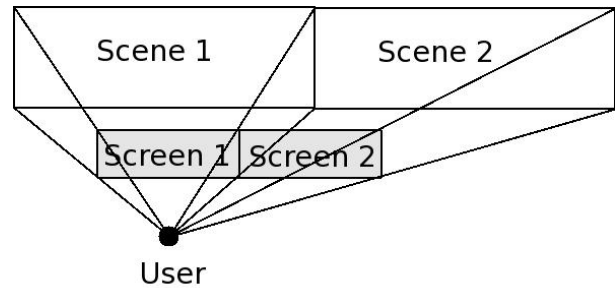


Fig. 6. Schematic representation of the VRJuggler display philosophy, here implemented on two screens (for detail see text). Objects positioned behind the screen are projected, dependent on their position relative to the user's viewing angle, creating the impression of realistic scenery.

As the display system is driven by a cluster of computers, individual processors must render corresponding aspects of the 'virtual world' in synchrony with their 'neighbours', and respond to commands from user-controlled input devices. Device handling, computation of viewing position, direction, and magnification, as well as control of rendering, are implemented using an open source Virtual Reality platform (*VRJuggler*; <http://www.vrjuggler.org/>). The basic premise of the *VRJuggler* world is that it includes a user, a screen, and objects in the virtual world (Fig. 6). Rather than moving the camera to look at the world (as is typically done in computer games), the world is moved 'outside' the projection window. Given that the user's position remains fixed relative to the window, this approach creates the impression of 'real' 3D perspectives when objects move across the screen.

User control of an application like this requires input devices that are mobile and, ideally, at least partially analogue. Our display system is navigated using a wireless gamepad (similar to a Playstation-2 controller), which provides two analogue joysticks and fourteen programmable buttons. This enables the user to move, rotate, zoom and cut through the data space, using intuitive controls, whilst standing right in front of the display wall.

The major advantage of using a high resolution display is that very fine detail can be seen without losing the contextual information about where in the dataset one is. Orientation is further aided by a 'thumbnail' that occupies four screens in the top-left corner of the powerwall (Fig. 7). The thumbnail provides an indication of where the image on the large-screen area is located, relative to the whole organ (which is always displayed centrally on the thumbnail). When the view 'enters' the tissue, a cutting plane is applied to the thumbnail in order to provide positional information, while projection of reduced-resolution MRI slices 'behind' the cutting plane provide substrate information. Figure 8 shows a detail view of the left ventricular chamber, as it would be experienced by the user.

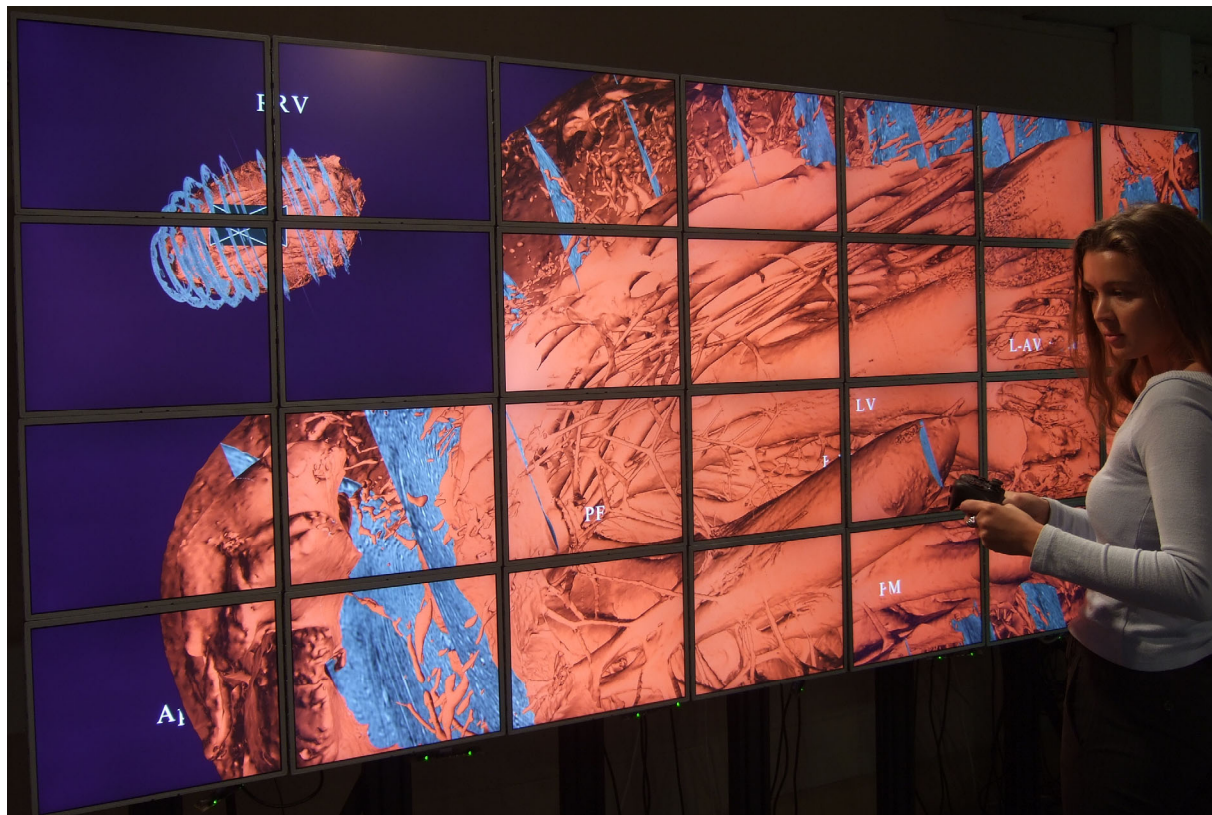


Fig. 7. High resolution multi-panel display wall, showing the left ventricle of the heart in cross-section, viewed from the septum, and the ‘thumb-nail’ orientation aid in top left corner. The data space is navigated using a wireless standard game console controller pad.

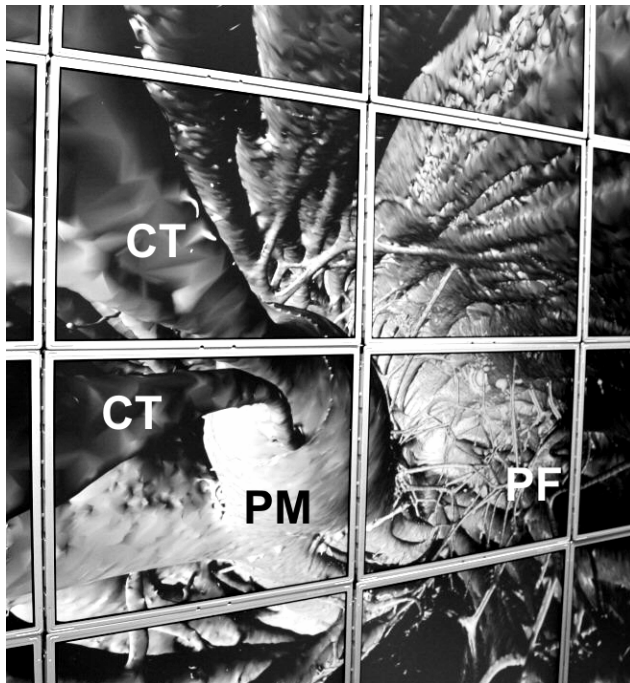


Fig. 8. Detail of the 53 megapixel display, showing baso-apical inside view of left ventricle with chordae tendinae (CT) projecting upwards from papillary muscle (PM). Note visibility of fine detail, such as free-running Purkinje fibres (PF).

VI. CONCLUSION

Novel visualization environments are needed to realise the vast potential of modern high-resolution non-invasive imaging modalities. These tools make examination of complex organ structures possible by showing 3D histo-anatomical features in connected data sets at variable, user-defined resolution. Here, we describe a demonstration system for interactive visualization of large cardiac data volumes through accurate surface rendering. Pre-processing of the data makes this application fast enough for real-time rendering on standard commodity hardware. The use of a high resolution display wall combines projection of fine detail with contextual information, which is further enhanced by thumbnail projection and display of alphanumeric labels.

REFERENCES

- [1] AM Katz and PB Katz. ‘Homogeneity Out of Heterogeneity.’ *Circulation* 1989/79:712-717.
- [2] RAB Burton, G Plank, JE Schneider, V Grau, H Ahammer, SL Keeling, J Lee, NP Smith, D Gavaghan, N Trayanova and P Kohl. ‘Three-Dimensional Models of Individual Cardiac Histoanatomy: Tools and Challenges’ *Ann N Y Acad Sci* 2006/1080:301-319.
- [3] S Ordas HC van Assen, L Boisrobert, M Laucelli, J Puente, BPF Lelieveldt, AF Frangi: ‘Statistical Modeling and Segmentation in Cardiac MRI Using a Grid Computing Approach.’ *Lecture Notes in Computer Science* 2005/3470: 3-15.
- [4] J Hodrien, J Wood and R. Ruddle. ‘The design and implementation of a 50 million pixel Powerwall display’, VizNet report, available online at <http://www.comp.leeds.ac.uk/viznet/>, 2007.